

Published in final edited form as:

Nat Immunol. 2016 June ; 17(6): 721–727. doi:10.1038/ni.3424.

TCR signal strength controls thymic differentiation of discrete proinflammatory $\gamma\delta$ T cell subsets

Miguel Muñoz-Ruiz^{1,2}, Julie C. Ribot², Ana R. Grosso², Natacha Gonçalves-Sousa², Ana Pamplona², Daniel J. Pennington³, José R. Regueiro¹, Edgar Fernández-Malavé^{#1}, and Bruno Silva-Santos^{#2}

¹Department of Immunology, School of Medicine, Complutense University, Madrid, Spain.

²Instituto de Medicina Molecular, Faculdade de Medicina, Universidade de Lisboa, Lisbon, Portugal.

³Blizard Institute, Barts and The London School of Medicine, Queen Mary University of London, London, United Kingdom.

These authors contributed equally to this work.

Abstract

The murine thymus produces discrete $\gamma\delta$ T cell subsets making either interferon- γ (IFN- γ) or interleukin 17 (IL-17), but the role of the TCR in this developmental process remains controversial. Here we show that mice haploinsufficient for both *Cd3g* and *Cd3d* (CD3DH, for CD3 double haploinsufficient) have reduced TCR expression and signaling strength selectively on $\gamma\delta$ T cells. CD3DH mice had normal numbers and phenotype of $\alpha\beta$ thymocyte subsets but impaired differentiation of fetal V γ 6⁺ (but not V γ 4⁺) IL-17-producing $\gamma\delta$ T cells and a marked depletion of IFN- γ -producing CD122⁺ NK1.1⁺ $\gamma\delta$ T cells throughout ontogeny. Adult CD3DH mice showed reduced peripheral IFN- γ ⁺ $\gamma\delta$ T cells and were resistant to experimental cerebral malaria. Thus, TCR signal strength within specific thymic developmental windows is a major determinant of the generation of proinflammatory $\gamma\delta$ T cell subsets and their impact on pathophysiology.

Proinflammatory cytokines orchestrate protective immune responses to pathogens and tumors, but are also responsible for tissue-damaging inflammation and autoimmunity. Among various cellular sources, $\gamma\delta$ T cells have emerged as major producers of interferon- γ (IFN- γ) and/ or interleukin 17 (IL-17) in several diseases. On one hand, IFN- γ production by $\gamma\delta$ T cells underlies protective responses to infections¹, as well as tumor immunity², but,

Users may view, print, copy, and download text and data-mine the content in such documents, for the purposes of academic research, subject always to the full Conditions of use: http://www.nature.com/authors/editorial_policies/license.html#terms

Correspondence should be addressed to B.S.-S. (bssantos@medicina.ulisboa.pt) or E.F.-M. (edferman@med.ucm.es).

Author contributions

Designed research: MMR, BSS, EFM, JRR, DJP

Performed experiments: MMR, JCR, ARG, NGS, AP

Supervised research and wrote the manuscript: BSS, EFM, JRR

Accession codes. Microarray data, GSE71637.

Conflicts of interest

The authors declared no conflicts of interest.

conversely, it is associated with susceptibility to severe malaria³. On the other hand, IL-17 secretion by $\gamma\delta$ T cells is a key defense mechanism against various bacterial infections, such as *Staphylococcus aureus*⁴ or *Listeria monocytogenes*^{4, 5}, but is also a critical component of inflammatory and autoimmune syndromes like psoriasis⁶⁻⁸, colitis⁹, chronic granulomatous disease¹⁰, ischemic brain inflammation¹¹ and experimental autoimmune encephalomyelitis¹²⁻¹⁴.

The non-redundant roles of IFN- γ -producing (IFN- γ^+) and IL-17-producing (IL-17⁺) $\gamma\delta$ T cells are tightly linked to “developmental pre-programming” in the murine thymus¹⁵. Whereas conventional effector CD4⁺ T cells differentiate in peripheral lymphoid organs in response to antigen and additional environmental cues, $\gamma\delta$ T cells complete their functional maturation in the thymus. On the basis of CD27 and CCR6 expression, the murine thymus generates discrete populations of IFN- γ^+ and IL-17⁺ $\gamma\delta$ T cells^{16, 12, 17}. Importantly, these subpopulations have different functions: for example, CD27⁻ IL-17⁺ $\gamma\delta$ T cells promote tumor cell growth^{18, 19} whereas CD27⁺ IFN- γ^+ $\gamma\delta$ T cells inhibit it^{2, 20}. It is therefore critical to understand how distinct functional $\gamma\delta$ T cell subsets are generated and regulated.

Given its pivotal role in thymocyte development and selection, the T cell receptor (TCR) is a likely determinant of the functional differentiation of $\gamma\delta$ T cells¹⁵. It was shown that T10/T22 tetramer-specific $\gamma\delta$ T cells, which account for ~0.4% of peripheral $\gamma\delta$ T cells, produced IL-17 or IFN- γ in the absence or presence, respectively, of thymic T10/T22 expression¹². Consistent with this, thymic selection drives dendritic epidermal T cells (DETC) that populate the mouse epidermis towards IFN- γ but away from IL-17 production²¹. However, SKG mice, which are hypomorphic for the TCR signal-transducing kinase ZAP70, retaining only 10% of its signaling ability, showed impaired development of IL-17⁺ $\gamma\delta$ T cells²². As such, the role of TCR signal “strength” in the development of proinflammatory $\gamma\delta$ T cell subsets remains unclear.

TCR signal strength is known to control the earliest stage of $\gamma\delta$ T cell development, i.e., lineage commitment²³. The manipulation of signal transduction in TCR transgenic T cells influenced the $\gamma\delta$ versus $\alpha\beta$ thymocyte fate^{24, 25}, with $\gamma\delta$ T cells requiring stronger TCR signaling than $\alpha\beta$ T cells to develop. However, the impact on subsequent maturation of $\gamma\delta$ T cells, particularly IFN- γ^+ versus IL-17⁺ $\gamma\delta$ T cells, was not assessed. On the other hand, models based on a single transgenic TCR may not be ideal to answer this question, because $\gamma\delta$ T cell development is tightly linked to the dynamics of TCR rearrangements during ontogeny. Indeed, “developmental waves” with distinct TCR gene usage populate different peripheral tissues, and distinct TCR γ chain variable region (V γ) repertoires can have significant biases towards either IFN- γ or IL-17 production^{16, 26}. For example, of the two main $\gamma\delta$ T cell subsets in peripheral lymphoid organs, V γ 1⁺ T cells preferentially secrete IFN- γ , whereas V γ 4⁺ T cells are biased towards IL-17^{16, 26}. In addition, V γ 5⁺ T cells generated around embryonic days E15-E16 do not secrete IL-17, while this cytokine is abundantly produced by V γ 6⁺ T cells that differentiate at E17-E18. Moreover, in-depth transcriptional profiling of $\gamma\delta$ thymocyte subsets by the Immunological Genome Project (www.immgen.org) demonstrated a divergence between the transcriptional networks of IL-17 -biased V γ 6⁺ and V γ 4⁺ T cells versus IFN- γ -biased V γ 5⁺ and V γ 1⁺ T cells^{27, 28}.

The association between certain $\gamma\delta$ TCR repertoires and differential IFN- γ or IL-17 production²⁶ suggests that TCR signaling is a major determinant of the functional differentiation of $\gamma\delta$ T cells in the thymus. However, testing this hypothesis has been hampered by the lack of mouse models that specifically interfere with TCR $\gamma\delta$ signaling *in vivo*. Here we describe a selective defect in the surface expression of TCR $\gamma\delta$, but not TCR $\alpha\beta$, in *Cd3d*^{+/-} *Cd3g*^{+/-} mice (CD3DH, for CD3 double haploinsufficient), and show that reduced TCR $\gamma\delta$ signaling impacts on the differentiation of discrete subsets of IFN- γ and IL-17-producing $\gamma\delta$ T cells during thymic ontogeny with pathological consequences.

Results

Cd3d^{+/-} *Cd3g*^{+/-} mice show reduced TCR signaling in $\gamma\delta$ T cells

During the screening of various lines of (single or double) haploinsufficient CD3 mutants, we observed that *Cd3d*^{+/-} *Cd3g*^{+/-} mice (hereafter CD3DH, for double haploinsufficient) had markedly lower cell surface expression of TCR $\gamma\delta$ and CD3 ϵ (Fig. 1a,b) and reduced $\gamma\delta$ thymocyte numbers (Fig. 1c). This reduction was not observed in single haploinsufficient, *Cd3d*^{+/-} or *Cd3g*^{+/-} mice (Supplementary Fig. 1a), and was more severe than that observed in CD3 δ -deficient mice²⁹ (Supplementary Fig. 1b). The reduced numbers of $\gamma\delta$ thymocytes in CD3DH mice were not due to increased cell death (Supplementary Fig. 1c), suggesting that lower TCR $\gamma\delta$ expression impaired $\gamma\delta$ T cell development, as reported in transgenic models^{24, 25}. CD3DH $\gamma\delta$ thymocytes remained mostly CD4⁻ CD8⁻ (data not shown), thus excluding diversion into the $\alpha\beta$ lineage. On the other hand, TCR $\alpha\beta$ expression was not affected, and $\alpha\beta$ thymocyte development proceeded normally in CD3DH mice (Fig. 1d-f). Consistent with normal TCR $\alpha\beta$ signaling and selection, the generation of agonist-selected Foxp3⁺ CD4⁺ and CD1d-restricted NKT cells was similar to wild-type mice (Supplementary Fig. 1d,e).

To characterize the downstream effects of reduced TCR $\gamma\delta$ expression we assessed the expression of agonist selection markers, namely CD73, a signature of TCR $\gamma\delta$ signaling during thymic development³⁰, and CD5, a stable indicator of TCR signal strength³¹, as well as the maturation markers CD122 and CD44^{12, 15, 17}. All were markedly reduced in $\gamma\delta$ thymocytes from CD3DH compared to wild-type mice (Fig. 1g). Upon TCR stimulation, the activation markers CD69 and CD25 were also decreased in peripheral (splenic) CD3DH $\gamma\delta$ T cells (Fig. 1h). Moreover, CD3DH $\gamma\delta$ T cells had lower TCR responsiveness in terms of ERK (Fig. 1i) and AKT (Supplementary Fig. 2a) activation or calcium mobilization (Supplementary Fig. 2b) compared to wild-type $\gamma\delta$ T cells. These data indicate that lower surface TCR $\gamma\delta$ expression in *Cd3d*^{+/-} *Cd3g*^{+/-} mice impairs signal transduction and downstream TCR-dependent processes.

To test whether the phenotype of $\gamma\delta$ T cells in CD3DH mice was cell-intrinsic, we established mixed (1:1) bone marrow (BM) chimeras by transferring CD3DH (Thy-1.2) and wild-type (Thy-1.1) whole BM cells into either TCR δ -deficient or RAG2-deficient hosts. In both hosts we observed reduced TCR $\gamma\delta$ expression in CD3DH-derived $\gamma\delta$ thymocytes (Fig. 1j), which consistently accounted for a minor fraction of the total $\gamma\delta$ thymocyte pool, compared to wild-type $\gamma\delta$ thymocytes. In contrast, $\alpha\beta$ thymocytes were evenly generated from CD3DH or wild-type precursors (Fig. 1k), indicating that CD3DH progenitors are

outcompeted by wild-type precursors for $\gamma\delta$, but not $\alpha\beta$ T cell development. Of note, this disadvantage could be compensated by using a 1:9 WT: CD3DH ratio (Supplementary Fig. 3), which indicated that CD3DH progenitors can generate $\gamma\delta$ thymocytes albeit with reduced potency compared to wild-type precursors. Thus, haploinsufficiency for both *Cd3d* and *Cd3g* results in lower TCR $\gamma\delta$ expression levels and signaling and reduced numbers of $\gamma\delta$ thymocytes.

Impaired differentiation of IL-17⁺ and IFN- γ ⁺ $\gamma\delta$ T cell subsets

We next analyzed the functional differentiation of $\gamma\delta$ T cell subsets. Development of CD27⁺ and CD27⁻ $\gamma\delta$ T cells was observed during the embryonic stages and continued into adulthood (Fig. 2a), as previously reported.¹⁶ Both IFN- γ ⁺ and IL-17⁺ $\gamma\delta$ thymocytes were observed in reduced frequencies in CD3DH compared to wild-type E18 embryos (Fig. 2b, c). Whereas the reduction in IFN- γ ⁺ $\gamma\delta$ thymocytes was maintained after birth into adulthood, the frequency of IL-17⁺ $\gamma\delta$ thymocytes in CD3DH mice normalized to wild-type levels between 1 and 6 weeks of age (Fig. 2b-d). This coincided with a switch in TCR V γ usage: most IL-17⁺ $\gamma\delta$ T cells are V γ 1⁻ V γ 4⁻ (validated as V γ 6⁺ by GL3/ 17D1 antibody staining as in¹⁸, not shown) in E18 embryos and neonates, and V γ 4⁺ from week 1 onwards (Fig. 2e). Of note, IL-17⁺ V γ 6⁺ cells are generated exclusively during embryonic life³². Importantly, only V γ 6⁺ but not V γ 4⁺ thymocytes showed reduced IL-17 production in CD3DH mice (Fig. 2f). These data suggest that the effector $\gamma\delta$ T cell subsets generated within distinct developmental windows, as marked by particular V γ usage, have distinct TCR signal strength requirements.

Transcriptional signatures of TCR signal strength in $\gamma\delta$ T cells

Because developmental programming of $\gamma\delta$ T cells is set at the transcriptional level^{27, 33, 34}, we performed transcriptome-wide analysis of sorted total $\gamma\delta$ thymocytes from CD3DH or wild-type mice at E18 of embryonic development or at 6-week of age. This analysis showed highly dynamic patterns of gene expression during ontogeny (Fig. 3a). Among the mRNAs upregulated in $\gamma\delta$ thymocytes from E18 to adult in wild-type mice, those linked to IFN- γ production were generally impaired in CD3DH $\gamma\delta$ thymocytes, such as *Nr4a3*, *Nr4a2* and *Bcl2a1*^{16, 34, 35}, the transcription factors *Egr2*, *Egr3* and *Id3*, which are major suppressors of the IL-17 differentiation pathway²¹, and *Nfkbiz* (which encodes the transcription factor I κ B ζ)³⁶, *Tnfrsf18* (encoding GITR), *Gp49a* and *Lilrb4* (encoding Gp49b)³⁷, which are involved in the regulation of IFN- γ production (Fig. 3a, Supplementary Fig. 4a).

On the other hand, key type 17 genes, such as *Il17a*, *Il17f* and *Il23r*^{13,33}, which are highly expressed in fetal $\gamma\delta$ thymocytes and reduced in adult $\gamma\delta$ thymocytes in wild-type mice, were downregulated in CD3DH $\gamma\delta$ thymocytes (Fig. 3a). Both wild-type and CD3DH $\gamma\delta$ thymocytes downregulated the embryonically rearranged TCRs, such as V γ 5 and V γ 6, as well as the transcription factor PLZF (encoded by *Zbtb16*), which is characteristic of fetal $\gamma\delta$ thymocytes²⁷ (Fig. 3a).

The type 17 signature genes *Sox 4* and *Sox13* (ref 27, 28) were greatly reduced in embryonic V γ 6⁺, but not V γ 4⁺ CD3DH (compared to wild-type) thymocytes (Supplementary Fig. 4b), indicating that the IL-17⁺V γ 6⁺ and IL-17⁺V γ 4⁺ thymocyte subsets

have distinct developmental TCR signal strength requirements. Of note, the expression of *Tbx21* (which encodes T-bet) and *Rorc* (which encodes ROR γ t), which transcriptionally regulate *Ifng* and *Il17a* expression respectively, was not affected in CD3DH compared to wild-type $\gamma\delta$ thymocytes (data not shown).

Next, for a TCR-mediated gain-of-function approach, we stimulated total $\gamma\delta$ thymocytes from adult CD3DH or wild-type mice with saturating amounts of anti-CD3 ϵ mAb for 16 hours, to achieve crosslinking of all available TCR complexes on the cell surface. We observed an upregulation of *Egr2* and *Egr3* expression in wild-type $\gamma\delta$ thymocytes (Fig. 3b), consistent with their induction by strong TCR signals²¹. *Egr2* and *Egr3* upregulation was also observed in stimulated CD3DH $\gamma\delta$ thymocytes (Fig. 3b), suggesting that increasing $\gamma\delta$ TCR signaling can rescue the expression of IFN- γ -associated transcriptional signatures in CD3DH $\gamma\delta$ thymocytes. In addition, anti-CD3 ϵ mAb stimulation downregulated the type 17 signature genes, such as *Sox4*²⁸, *Il23r* and *Il1rl1*^{13, 33, 38}, in both wild-type and CD3DH $\gamma\delta$ thymocytes (Fig. 3b). Collectively, these data suggest that strong TCR signals are required to promote IFN- γ at the expense of IL-17 production by adult $\gamma\delta$ thymocytes.

CD3DH mice lack IFN- γ ^{hi} CD122⁺ NK1.1⁺ $\gamma\delta$ thymocytes

We next tested if the deficiency in IFN- γ expression in $\gamma\delta$ thymocytes from CD3DH mice involved the depletion of a specific $\gamma\delta$ T cell subset committed to IFN- γ production. Thus, we analyzed the expression of CD122 (ref¹²) and NK1.1 (ref^{17,30}), two markers previously associated with IFN- γ ⁺ $\gamma\delta$ T cells, on adult CD27⁺ $\gamma\delta$ T cells. We detected a CD122⁺ NK1.1⁺ $\gamma\delta$ T cell population in the wild-type thymus that was absent in CD3DH mice (Fig. 4a, b). CD122⁺ NK1.1⁻ $\gamma\delta$ T cells, likely precursors of CD122⁺ NK1.1⁺ $\gamma\delta$ T cells, were also reduced in the CD3DH thymus compared to wild-type (Fig. 4a). The V γ repertoire changed from V γ 4-biased to V γ 1-enriched between the CD122⁻ and the more mature CD122⁺ $\gamma\delta$ T cells in wild-type thymi (Fig. 4c), suggesting that TCR selection shapes the mature $\gamma\delta$ thymocyte pool. Furthermore, consistent with a requirement for strong TCR signaling, wild-type CD122⁺ NK1.1⁺ $\gamma\delta$ thymocytes had high expression of the selection markers CD44, CD73 and CD45RB, which were not detected on CD122⁻ $\gamma\delta$ thymocytes (Fig. 4d). Importantly, wild-type CD122⁺ NK1.1⁺ $\gamma\delta$ thymocytes had the highest expression of IFN- γ (Fig. 4d), suggesting that the high IFN- γ -producing $\gamma\delta$ T cells have a differentiation defect in CD3DH mice. Furthermore, in mixed WT:CD3DH BM chimeras, CD27⁺ CD122⁺ NK1.1⁺ $\gamma\delta$ thymocytes were exclusively generated from wild-type progenitors (Fig. 4e). This observation was made in both 1:1 and 1:9 chimeras (Fig. 4e), indicating a strong competitive disadvantage of CD3DH precursors along this developmental pathway.

We next aimed to rescue the generation of CD122⁺ NK1.1⁺ $\gamma\delta$ thymocytes in CD3DH mice by cross-linking their TCR complex *in vivo*. Intraperitoneal injection of the 17A2 antibody, which cross-links CD3 $\epsilon\gamma$ dimers, rescued CD122⁺ NK1.1⁺ $\gamma\delta$ thymocyte development in CD3DH mice, leading to frequencies similar to wild-type mice (Fig. 4f, g). Moreover, wild-type mice treated with 17A2 showed an increase in CD122⁺ NK1.1⁺ $\gamma\delta$ thymocytes compared to untreated wild-type mice (Fig. 4a, f). These data indicate that strong TCR

signaling promotes (and is required for) the development of the IFN- γ^{hi} CD27 $^{+}$ CD122 $^{+}$ NK1.1 $^{+}$ $\gamma\delta$ thymocyte subset.

Reduced IFN- γ^{+} $\gamma\delta$ splenocytes and resistance to cerebral malaria

We next investigated the consequences of reduced $\gamma\delta$ TCR signaling in CD3DH mice on peripheral $\gamma\delta$ T cells. Upon *ex vivo* PMA+ionomycin stimulation, CD3DH splenocytes showed reduced CD27 $^{+}$ IFN- γ^{+} but normal CD27 $^{-}$ IL-17 $^{+}$ $\gamma\delta$ T cell frequencies compared to wild-type splenocytes (Fig. 5a, b). In contrast, CD3DH CD4 $^{+}$ $\alpha\beta$ T cells differentiated normally into Th1 cells when activated in the presence of IL-12 (Supplementary Fig. 5), indicating that the IFN- γ defect of CD3DH mice was selective for $\gamma\delta$ T cells. Moreover, CD27 $^{+}$ CD122 $^{+}$ NK1.1 $^{+}$ CD44 $^{+}$ $\gamma\delta$ splenocytes were absent in CD3DH compared to wild-type mice (Fig. 5c-f). This was also observed in competitive WT:CD3DH BM chimeras, both at 1:1 and 1:9 ratios (Fig. 5e).

We next assessed the physiological importance of IFN- γ -producing $\gamma\delta$ T cells in a model of cerebral malaria, which in C57BL/6 mice induces IFN- γ -dependent pathology³⁹ and in both mice and humans³ requires a major contribution from $\gamma\delta$ T cells. We induced experimental cerebral malaria with *Plasmodium berghei* ANKA sporozoites, thus establishing a liver-stage infection before spreading to the blood, which is the symptomatic stage. Whereas wild-type mice presented an abundant IFN- γ^{+} $\gamma\delta$ T cell population in the spleen at day 5 post-infection (blood stage), this was markedly reduced in CD3DH mice (Fig. 5g), and associated with higher parasitemia (measured as % of infected red blood cells) compared to infected wild-type mice (Fig. 5h). Neurological symptoms appeared in wild-type mice around day 6 post-infection and became fatal in all animals by days 7-10 (Fig. 5i). By contrast, $\gamma\delta$ T cell-deficient (TCR δ -deficient), as well as most CD3DH mice remained healthy and survived (Fig. 5i). These data demonstrate that IFN- γ^{+} $\gamma\delta$ T cells make mice highly susceptible to fatal inflammatory syndromes like severe malaria.

Discussion

The reduced TCR $\gamma\delta$ expression on the surface of $\gamma\delta$ thymocytes in CD3DH mice allowed us to examine a diverse, polyclonal TCR $\gamma\delta$ repertoire, which is highly valuable given the association between specific TCR gene usage and functional differentiation biases²⁶. Our results suggest that distinct developmental $\gamma\delta$ T cell subsets defined by *TCRVG* rearrangement and *V γ* usage have distinct TCR signal strength requirements for differentiation into IFN- γ - or IL-17-producing cells.

CD3 δ was shown to be absent from mouse mature TCR $\gamma\delta$ complexes^{42, 43}, which raises the question how it impacts surface TCR $\gamma\delta$ expression. As we found no evidence for the presence of CD3 δ on the surface of $\gamma\delta$ thymocytes (data not shown), we are currently investigating the possibility that CD3 δ transiently participates in TCR $\gamma\delta$ assembly. Also, changes in the relative intracellular amounts of CD3 chains as observed in CD3DH mice could cause abnormal glycosylation of CD3 δ ^{44, 45} (data not shown) and/or CD3 γ ⁴⁶, which in turn could impair the assembly and stability of nascent TCR complexes, and ultimately their surface expression and signaling^{41, 46}. TCR signaling strength impacts thymic commitment to the $\alpha\beta$ versus $\gamma\delta$ lineages²³⁻²⁵. Consistent with this, CD3DH mice showed

reduced numbers of total $\gamma\delta$ thymocytes, including loss of CD122⁺ NK1.1⁺ $\gamma\delta$ T cells (expressing high IFN- γ levels). The number and frequencies of $\alpha\beta$ T cell subsets, including thymic regulatory (T_{reg}) and invariant NKT (iNKT) cells, was normal in CD3DH mice, although the repertoire of TCR $\alpha\beta$ ⁺ subpopulations was not assessed. However, the expression of the $\alpha\beta$ TCR was normal in developing CD3DH thymocytes, indicating that the reduction in TCR expression was specific to $\gamma\delta$ thymocytes.

Interestingly, whereas IL-17⁺ V γ 6⁺ cells were underrepresented in CD3DH mice, their IL-17⁺ V γ 4⁺ counterparts were not affected, consistent with distinct developmental requirements for the two IL-17-producing $\gamma\delta$ T cell subsets³². V γ 6⁺ thymocytes have been shown to outcompete V γ 4⁺ thymocytes when reconstituting the dermis of $\gamma\delta$ T cell-deficient mice⁸, and whereas fetal-derived (and thymically programmed) V γ 6⁺ T cells were shown to be resident in the dermis, adult BM-derived V γ 4⁺ T cells seem to depend on extrathymic signals to migrate to the skin. Thus, by differentially controlling tissue homing properties, thymic programming may determine the pathophysiological contributions of discrete $\gamma\delta$ T cell subsets. Consistent with this, V γ 4⁺ T cells represent the major source of IL-17 in psoriasis-like inflammation^{8, 32}, as well as in experimental autoimmune encephalomyelitis¹³ and collagen-induced arthritis⁴⁸, whereas V γ 6⁺ T cells are more frequent in *Listeria* infection⁵ and ovarian cancer¹⁸.

The observation that fetal-derived and adult IL-17-producing $\gamma\delta$ T cells have distinct TCR signaling requirements could not be obtained using the available (V γ 4-based) transgenic TCR $\gamma\delta$ models, and resolves previous controversies on the TCR (in)dependence of IL-17⁺ $\gamma\delta$ T cell development^{12, 21, 22, 28}. Namely, our data indicates that V γ 6⁺, but not V γ 4⁺, thymocytes depend on strong TCR signals for functional differentiation, which in turn warrants investigation into their respective ligand engagement requirements.

In addition to ligand engagement, distinct signaling cascades downstream of the TCR $\gamma\delta$ may differentially affect $\gamma\delta$ T cell subsets. It will be important to establish if TCR $\gamma\delta$ signaling is perceived mostly quantitatively or, rather, qualitatively based on the engagement of distinct signaling pathways, such as ERK-MAPK or PI3K-AKT (Nital Sumaria, B.S.-S. and D. J. P., unpublished results). Further downstream in cellular programming, our transcriptional analysis of fetal and adult total $\gamma\delta$ thymocytes stages showed that CD3DH $\gamma\delta$ thymocytes efficiently downregulated the IL-17 program, but were deficient in upregulating the IFN- γ pathway between fetal and adult stages. Particularly affected were the transcription factors *Egr2*, *Egr3* and *Id3*, which are induced by agonist TCR signaling^{21, 50}, and may be required to suppress a “default” ROR γ t-dependent IL-17 program and maximize IFN- γ production in $\gamma\delta$ thymocytes. This would be consistent with both the repression of the IL-17 pathway in V γ 5⁺ DETC development²¹ and the depletion, in CD3DH mice, of V γ 1-biased CD27⁺ CD122⁺ NK1.1⁺ $\gamma\delta$ T cells, the subset expressing the highest IFN- γ on a per cell basis.

Interestingly, the transcription factors that control *Ifng* and *Il17a* expression, T-bet and ROR γ t, were normally expressed in CD3DH $\gamma\delta$ T cell subsets, suggesting that the $\gamma\delta$ T cell differentiation phenotype in these mice derives from mechanisms downstream of T-bet or ROR γ t expression. This is in agreement with normal expression of these transcription factors in $\gamma\delta$ thymocytes deficient for the TCR signal transducer Itk²⁸. We therefore propose that a

major function of TCR $\gamma\delta$ signaling is to select preprogrammed precursors, which could resemble innate lymphoid cells (ILC), for differentiation into effector cells making IFN- γ or IL-17. Future studies on the functional similarities and differences between ILC and $\gamma\delta$ T cell subsets may contribute to understanding the evolutionary conservation of these innate-like lymphocytes and their therapeutic potential for infectious or inflammatory diseases and cancer²⁰.

Online methods

Mice

Adult mice were used at 4–8 weeks of age. Embryos were obtained by the setting up of timed pregnancies. C57BL/6 (WT) mice were from Charles River Laboratories. CD3 $\gamma^{-/-}$ mice have been previously described⁵¹, and were kindly given by Dr. D. Kappes (Fox Chase Cancer Center, Philadelphia). CD3 $\delta^{-/-}$ have been previously described²⁹ and were yield by Dr. I. Luescher (Ludwig Institute for Cancer Research, Lausanne). Double heterozygotes (CD3DH) were obtained by crossing CD3 $\gamma^{-/-}$ males with CD3 $\delta^{-/-}$ females. For the studies, both males and females were used. Mice were bred and maintained in the pathogen-free animal facilities of the Instituto de Medicina Molecular (Lisbon) and Animalario Universidad Complutense (Madrid). All experiments involving animals were done in compliance with the relevant laws and institutional guidelines.. Experimental procedures were ethically approved by the Ethics Committee for Animal Experimentation of Universidad Complutense and Comunidad de Madrid, and by the institutional animal welfare body – ORBEA-iMM – and by the DGAV (Portuguese competent authority for animal protection), all in accordance with Directive 2010/63/EU.

Bone marrow chimeras

Rag2^{-/-} or *Tcrd^{-/-}* mice were lethally irradiated (900 rad), and the next day injected intravenously with a total of 10^7 whole bone marrow cells of mixed (1:1 or 1:9) WT.Thy-1.1 and CD3DH.Thy-1.2 origin. Chimeras were kept on antibiotics-containing water (2% Bactrim; Roche) for the first 4 weeks post-irradiation. The hematopoietic compartment was allowed to reconstitute for 6 weeks before organs were harvested for flow cytometry analysis.

Cell preparations

Thymuses, lymph nodes and spleens were homogenized and washed in RPMI medium containing 10% (vol/vol) FCS. Splenocytes were depleted from erythrocytes using the Red Blood Cell Lysis buffer 1x (Biolegend).

Monoclonal antibodies

Listed in Supplementary Table 1.

Flow cytometry and cell sorting

For cell surface staining, thymocytes, erythrocyte-depleted splenocytes or lymph node cells were incubated 30 min with saturating concentrations of mAbs identified above. For

intracellular cytokine staining, cells were stimulated with PMA (phorbol 12-myristate 13-acetate) (50ng/mL) and ionomycin (1µg/mL), in the presence of Brefeldin A (10µg/mL) (all from Sigma) for 4h at 37°C. Cells were stained for the identified above cell surface markers, fixed 30min at 4°C and permeabilized with the Foxp3/Transcription Factor Staining Buffer set (eBioscience) in the presence of anti-CD16/CD32 (93) (eBioscience) for 15 min at 4°C, and finally incubated for 1h at room temperature with identified above cytokine-specific Abs in permeabilization buffer. Samples were acquired using FACSFortessa (BD Biosciences). Data were analysed using FlowJo software (Tree Star). Live indicated subsets were electronically sorted when indicated using FACSARIA (BD Biosciences).

Cell culture

For early activation markers, cells were incubated for 24h on plate-bound anti-CD3ε (10 mg/ml) and analyzed by flow cytometry. For phosphorylated molecules downstream of TCR vs isotype-matched control antibody, sorted lymph node cells were stimulated for 5 min with soluble anti-CD3ε (10 µg/ml) then fixed 30min at 4°C and permeabilized with the Foxp3/Transcription Factor Staining Buffer set (eBioscience) in the presence of anti CD16/CD32 Fc Block (93) (eBioscience) for 30min at room temperature, and finally incubated for 1h at room temperature with identified above anti-p-ERK Abs in permeabilization buffer. For Th1 polarization CD4+ αβ T cells were isolated by flow cytometry and incubated for 4 days on plate-bound anti-CD3ε and anti-CD28 (5ng/ml each). When indicated (Th1 cocktail), the following cytokines and neutralizing antibody were added to the culture milieu: IL-2 (10 ng/ml; Preprotech), IL-12 (50 ng/ml; Preprotech) and anti-IL-4 (11B11) (10 µg/mL; eBiosciences).

Malaria infection

Mice were infected as described⁵².

RNA Isolation, cDNA Production, and Real-Time PCR

Total RNA was extracted using the RNeasy Mini kit (Qiagen) according to the manufacturer's instructions. Concentration and purity were determined using the NanoDrop ND-1000 spectrophotometer (Thermo Scientific). Total RNA was reverse transcribed into cDNA using a Transcriptor High Fidelity cDNA Synthesis kit (Roche). Quantitative real-time PCR was performed on ViiA 7 Real-Time PCR system (Applied Biosystems; Life Technologies). Primers were either designed manually or by using the Universal ProbeLibrary Assay Design Center from Roche (www.roche-applied-science.com). Sequences are available upon request. Analysis of the quantitative PCR results was performed using the ViiA 7 software v1.2 (Applied Biosystems; Life Technologies).

Microarray

Accession code GSE71637. All the microarray data analysis was done using R and several packages available from CRAN⁵³ and Bioconductor⁵⁴. The raw data (CEL files) were normalized and summarized with the Robust MultiArray Average method implemented in the 'oligo' package⁵⁵. Variations in gene expression levels were determined using 'limma'

package⁵⁶ and only genes with fold-change higher than 2 were considered for downstream analysis.

Statistical analysis

The statistical significance of differences between populations was assessed with the Student's t-test; P values of less than 0.05 were considered significant. Animal sample size was chosen to ensure significance of t-test. No animals were excluded. No randomization or blinding was performed. Data met normal distribution with similar variance between groups.

Supplementary Material

Refer to Web version on PubMed Central for supplementary material.

Acknowledgements

We thank K. Serre, J. Martins, N. Schmolka, A. Amorim, V. Z. Luís and M. M. Mota (all IMM Lisboa); and B. Garcillán, D. de Juan, M. Mazariegos, M. Sanz-Rodríguez and S. Diaz-Castroverde (U. Complutense) for help and advice; A. Hayday (King's College London) for insightful discussions; and the staff of our animal and flow cytometry facilities for technical assistance. This work was funded by the European Research Council (StG_260352 and CoG_646701) to B.S.-S.; MINECO (SAF2011-24235 and BES-2012-055054), CAM (S2010/BMD-2316/2326) and Lair (2012/0070) to J.R.R.; and FIS PI11/02198 and MINECO SAF2014-54708-R to E.F.-M.

References

1. Wang T, et al. IFN-gamma-producing gamma delta T cells help control murine West Nile virus infection. *J Immunol.* 2003; 171:2524–2531. [PubMed: 12928402]
2. Gao Y, et al. Gamma delta T cells provide an early source of interferon gamma in tumor immunity. *J Exp Med.* 2003; 198:433–442. [PubMed: 12900519]
3. Jagannathan P, et al. Loss and dysfunction of Vdelta2(+) gammadelta T cells are associated with clinical tolerance to malaria. *Sci Transl Med.* 2014; 6:251ra117.
4. Cho JS, et al. IL-17 is essential for host defense against cutaneous *Staphylococcus aureus* infection in mice. *J Clin Invest.* 2010; 120:1762–1773. [PubMed: 20364087]
5. Sheridan BS, et al. gammadelta T cells exhibit multifunctional and protective memory in intestinal tissues. *Immunity.* 2013; 39:184–195. [PubMed: 23890071]
6. Cai Y, et al. Pivotal role of dermal IL-17-producing gammadelta T cells in skin inflammation. *Immunity.* 2011; 35:596–610. [PubMed: 21982596]
7. Pantelyushin S, et al. Rorgammat+ innate lymphocytes and gammadelta T cells initiate psoriasiform plaque formation in mice. *J Clin Invest.* 2012; 122:2252–2256. [PubMed: 22546855]
8. Cai Y, et al. Differential developmental requirement and peripheral regulation for dermal Vgamma4 and Vgamma6T17 cells in health and inflammation. *Nat Commun.* 2014; 5:3986. [PubMed: 24909159]
9. Park SG, et al. T regulatory cells maintain intestinal homeostasis by suppressing gammadelta T cells. *Immunity.* 2010; 33:791–803. [PubMed: 21074460]
10. Romani L, et al. Defective tryptophan catabolism underlies inflammation in mouse chronic granulomatous disease. *Nature.* 2008; 451:211–215. [PubMed: 18185592]
11. Shichita T, et al. Pivotal role of cerebral interleukin-17-producing gammadeltaT cells in the delayed phase of ischemic brain injury. *Nat Med.* 2009; 15:946–950. [PubMed: 19648929]
12. Jensen KD, et al. Thymic selection determines gammadelta T cell effector fate: antigen-naïve cells make interleukin-17 and antigen-experienced cells make interferon gamma. *Immunity.* 2008; 29:90–100. [PubMed: 18585064]

13. Sutton CE, et al. Interleukin-1 and IL-23 induce innate IL-17 production from gammadelta T cells, amplifying Th17 responses and autoimmunity. *Immunity*. 2009; 31:331–341. [PubMed: 19682929]
14. Petermann F, et al. gammadelta T cells enhance autoimmunity by restraining regulatory T cell responses via an interleukin-23-dependent mechanism. *Immunity*. 2010; 33:351–363. [PubMed: 20832339]
15. Prinz I, Silva-Santos B, Pennington DJ. Functional development of gammadelta T cells. *Eur J Immunol*. 2013; 43:1988–1994. [PubMed: 23928962]
16. Ribot JC, et al. CD27 is a thymic determinant of the balance between interferon-gamma- and interleukin 17-producing gammadelta T cell subsets. *Nat Immunol*. 2009; 10:427–436. [PubMed: 19270712]
17. Haas JD, et al. CCR6 and NK1.1 distinguish between IL-17A and IFN-γ-producing gammadelta effector T cells. *Eur J Immunol*. 2009; 39:3488–3497. [PubMed: 19830744]
18. Rei M, et al. Murine CD27(-) Vgamma6(+) gammadelta T cells producing IL-17A promote ovarian cancer growth via mobilization of protumor small peritoneal macrophages. *Proc Natl Acad Sci U S A*. 2014; 111:E3562–3570. [PubMed: 25114209]
19. Wu P, et al. gammadeltaT17 cells promote the accumulation and expansion of myeloid-derived suppressor cells in human colorectal cancer. *Immunity*. 2014; 40:785–800. [PubMed: 24816404]
20. Silva-Santos B, Serre K, Norell H. Gamma-delta T cells in cancer. *Nat Rev Immunol*. 2015; 15:683–691. [PubMed: 26449179]
21. Turchinovich G, Hayday AC. Skint-1 identifies a common molecular mechanism for the development of interferon-gamma-secreting versus interleukin-17-secreting gammadelta T cells. *Immunity*. 2011; 35:59–68. [PubMed: 21737317]
22. Wencker M, et al. Innate-like T cells straddle innate and adaptive immunity by altering antigen-receptor responsiveness. *Nat Immunol*. 2014; 15:80–87. [PubMed: 24241693]
23. Ciofani M, Zuniga-Pflucker JC. Determining gammadelta versus alphabeta T cell development. *Nat Rev Immunol*. 2010; 10:657–663. [PubMed: 20725107]
24. Haks MC, et al. Attenuation of gammadeltaTCR signaling efficiently diverts thymocytes to the alphabeta lineage. *Immunity*. 2005; 22:595–606. [PubMed: 15894277]
25. Hayes SM, Li L, Love PE. TCR signal strength influences alphabeta/gammadelta lineage fate. *Immunity*. 2005; 22:583–593. [PubMed: 15894276]
26. O'Brien RL, Born WK. gammadelta T cell subsets: a link between TCR and function? *Semin Immunol*. 2010; 22:193–198. [PubMed: 20451408]
27. Narayan K, et al. Intrathymic programming of effector fates in three molecularly distinct gammadelta T cell subtypes. *Nat Immunol*. 2012; 13:511–518. [PubMed: 22473038]
28. Malhotra N, et al. A network of high-mobility group box transcription factors programs innate interleukin-17 production. *Immunity*. 2013; 38:681–693. [PubMed: 23562159]
29. Dave VP, et al. CD3 delta deficiency arrests development of the alpha beta but not the gamma delta T cell lineage. *EMBO J*. 1997; 16:1360–1370. [PubMed: 9135151]
30. Coffey F, et al. The TCR ligand-inducible expression of CD73 marks gammadelta lineage commitment and a metastable intermediate in effector specification. *J Exp Med*. 2014; 211:329–343. [PubMed: 24493796]
31. Azzam HS, et al. CD5 expression is developmentally regulated by T cell receptor (TCR) signals and TCR avidity. *J Exp Med*. 1998; 188:2301–2311. [PubMed: 9858516]
32. Haas JD, et al. Development of interleukin-17-producing gammadelta T cells is restricted to a functional embryonic wave. *Immunity*. 2012; 37:48–59. [PubMed: 22770884]
33. Schmolka N, et al. Epigenetic and transcriptional signatures of stable versus plastic differentiation of proinflammatory gammadelta T cell subsets. *Nat Immunol*. 2013; 14:1093–1100. [PubMed: 23995235]
34. Schmolka N, Wencker M, Hayday AC, Silva-Santos B. Epigenetic and transcriptional regulation of gammadelta T cell differentiation: Programming cells for responses in time and space. *Semin Immunol*. 2015; 27:19–25. [PubMed: 25726512]
35. Silva-Santos B, Pennington DJ, Hayday AC. Lymphotoxin-mediated regulation of gammadelta cell differentiation by alphabeta T cell progenitors. *Science*. 2005; 307:925–928. [PubMed: 15591166]

36. Kannan Y, et al. IkappaBzeta augments IL-12- and IL-18-mediated IFN- γ production in human NK cells. *Blood*. 2011; 117:2855–2863. [PubMed: 21224476]
37. Gu X, et al. The gp49B1 inhibitory receptor regulates the IFN- γ responses of T cells and NK cells. *J Immunol*. 2003; 170:4095–4101. [PubMed: 12682239]
38. Ribot JC, et al. Cutting edge: adaptive versus innate receptor signals selectively control the pool sizes of murine IFN- γ - or IL-17-producing gammadelta T cells upon infection. *J Immunol*. 2010; 185:6421–6425. [PubMed: 21037088]
39. Rudin W, Favre N, Bordmann G, Ryffel B. Interferon-gamma is essential for the development of cerebral malaria. *Eur J Immunol*. 1997; 27:810–815. [PubMed: 9130629]
40. Chien YH, Meyer C, Bonneville M. gammadelta T cells: first line of defense and beyond. *Annu Rev Immunol*. 2014; 32:121–155. [PubMed: 24387714]
41. Hayes SM, Love PE. Distinct structure and signaling potential of the gamma delta TCR complex. *Immunity*. 2002; 16:827–838. [PubMed: 12121664]
42. Hayes SM, Love PE. Stoichiometry of the murine gammadelta T cell receptor. *J Exp Med*. 2006; 203:47–52. [PubMed: 16418397]
43. Siegers GM, et al. Different composition of the human and the mouse gammadelta T cell receptor explains different phenotypes of CD3gamma and CD3delta immunodeficiencies. *J Exp Med*. 2007; 204:2537–2544. [PubMed: 17923503]
44. Zapata DA, et al. Conformational and biochemical differences in the TCR.CD3 complex of CD8(+) versus CD4(+) mature lymphocytes revealed in the absence of CD3gamma. *J Biol Chem*. 1999; 274:35119–35128. [PubMed: 10574994]
45. Fernandez-Malave E, et al. Overlapping functions of human CD3delta and mouse CD3gamma in alphabeta T-cell development revealed in a humanized CD3gamma-mouse. *Blood*. 2006; 108:3420–3427. [PubMed: 16888097]
46. Hayes SM, et al. Activation-induced modification in the CD3 complex of the gammadelta T cell receptor. *J Exp Med*. 2002; 196:1355–1361. [PubMed: 12438426]
47. Jin Y, et al. Cutting edge: Intrinsic programming of thymic gammadeltaT cells for specific peripheral tissue localization. *J Immunol*. 2010; 185:7156–7160. [PubMed: 21068400]
48. Roark CL, et al. Exacerbation of collagen-induced arthritis by oligoclonal, IL-17-producing gamma delta T cells. *J Immunol*. 2007; 179:5576–5583. [PubMed: 17911645]
49. Mahtani-Patching J, et al. PreTCR and TCRgammadelta signal initiation in thymocyte progenitors does not require domains implicated in receptor oligomerization. *Sci Signal*. 2011; 4:ra47. [PubMed: 21775286]
50. Seiler MP, et al. Elevated and sustained expression of the transcription factors Egr1 and Egr2 controls NKT lineage differentiation in response to TCR signaling. *Nat Immunol*. 2012; 13:264–271. [PubMed: 22306690]
51. Haks MC, Krimpenfort P, Borst J, Kruisbeek AM. The CD3gamma chain is essential for development of both the TCRalphabeta and TCRgammadelta lineages. *EMBO J*. 1998; 17:1871–1882. [PubMed: 9524111]
52. Liehl P, et al. Host-cell sensors for Plasmodium activate innate immunity against liver-stage infection. *Nat Med*. 2014; 20:47–53. [PubMed: 24362933]
53. Team RA. A language and environment for statistical computing. Vienna, Austria. 2011
54. Huber W, et al. Orchestrating high-throughput genomic analysis with Bioconductor. *Nat Methods*. 2015; 12:115–121. [PubMed: 25633503]
55. Carvalho BS, Irizarry RA. A framework for oligonucleotide microarray preprocessing. *Bioinformatics*. 2010; 26:2363–2367. [PubMed: 20688976]
56. Ritchie ME, et al. limma powers differential expression analyses for RNA-sequencing and microarray studies. *Nucleic Acids Res*. 2015; 43:e47. [PubMed: 25605792]

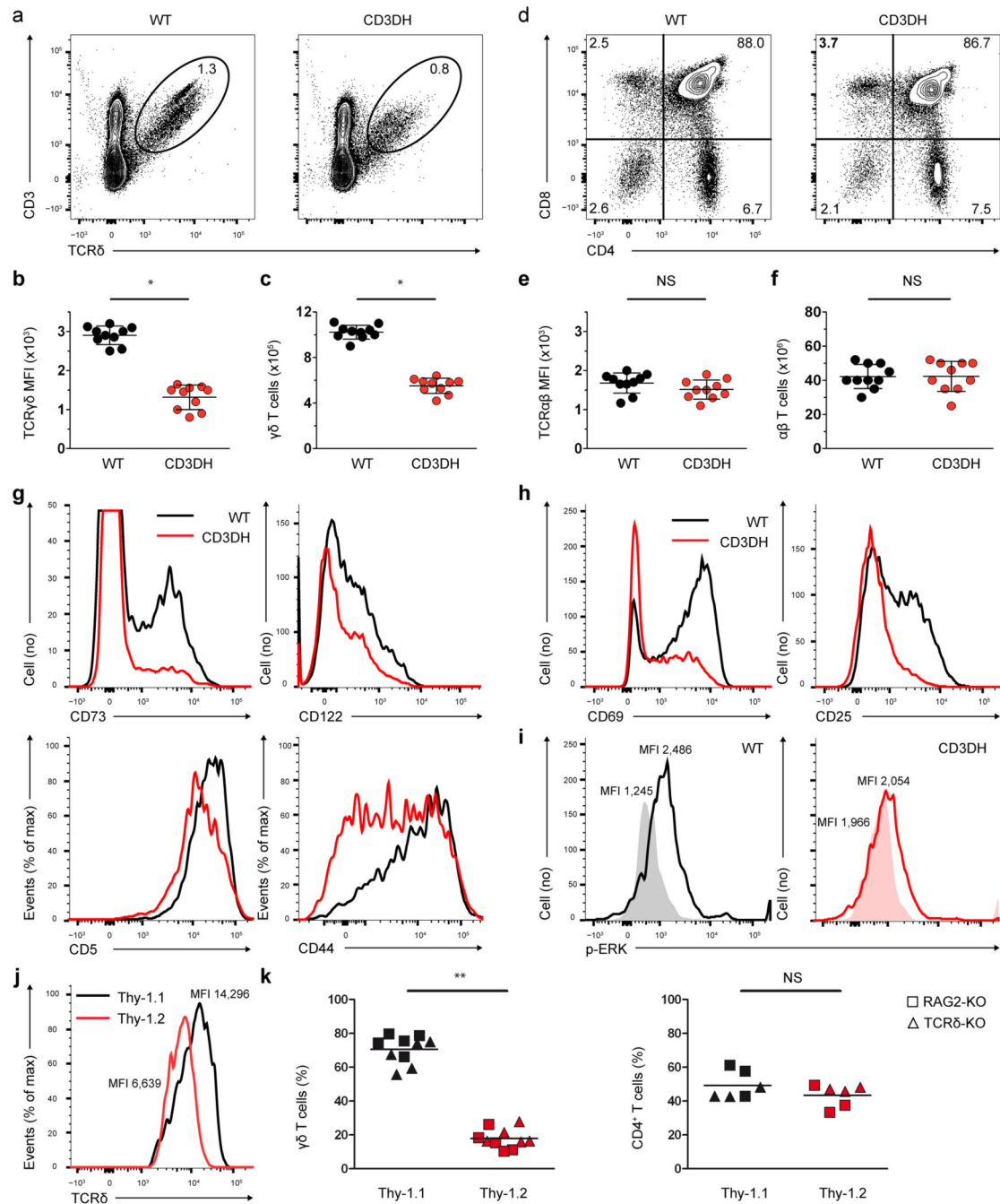


Figure 1. $\gamma\delta$ T cells from CD3DH mice show reduced TCR $\gamma\delta$ expression and signaling

(a) Flow cytometry showing the CD3 ϵ vs TCR δ phenotype of thymocytes from one-week old wild-type (WT) or *Cd3g^{+/-} Cd3d^{+/-}* (CD3DH) mice ($n = 10$ per group). Numbers within outlined areas or quadrants indicate % cells in each throughout. (b-f) TCR $\gamma\delta$ MFI (b) and $\gamma\delta$ thymocyte numbers (c) gated as in (a), CD8 vs CD4 phenotype of thymocytes ($n = 3$ per group of adult mice) (d), TCR $\alpha\beta$ MFI (e) and absolute numbers of TCR β^+ CD3 $^+$ thymocytes (f). (g-i) Flow cytometry showing expression of the indicated agonist selection and maturation markers in gated TCR δ^+ CD3 $^+$ CD27 $^+$ thymocytes (g), of CD69 and CD25 in

sorted $\text{TCR}\delta^+\text{CD}3^+\text{CD}27^+$ spleen cells stimulated with plate-coated $\alpha\text{-CD}3\epsilon$ mAb for 24h (h), of phosphorylated Erk1/Erk2 (empty histograms) vs isotype-matched background staining (filled histograms) in sorted $\text{TCR}\delta^+\text{CD}3^+\text{CD}27^+$ lymph node cells stimulated for 5 min with soluble $\alpha\text{-CD}3\epsilon$ mAb (i). Data are representative of 3 independent experiments. **(j, k)** Flow cytometry showing comparative $\text{TCR}\gamma\delta$ MFI (j) and Thy-1.1 (WT-derived) vs Thy-1.2 (CD3DH-derived) fractions among gated $\text{TCR}\delta^+\text{CD}3^+$ and $\text{CD}4^+\text{CD}3^+$ thymocytes (k) from 1:1 mixed WT:CD3DH bone marrow chimeras. Each symbol indicates one host, either $\text{RAG}2^{-/-}$ (squares) or $\text{TCR}\delta^{-/-}$ (triangles). In (b,c) and (e,f), dots represent individuals and horizontal lines mean \pm s.d. NS, not significant; $*P < 0.01$ (Student's t-test).

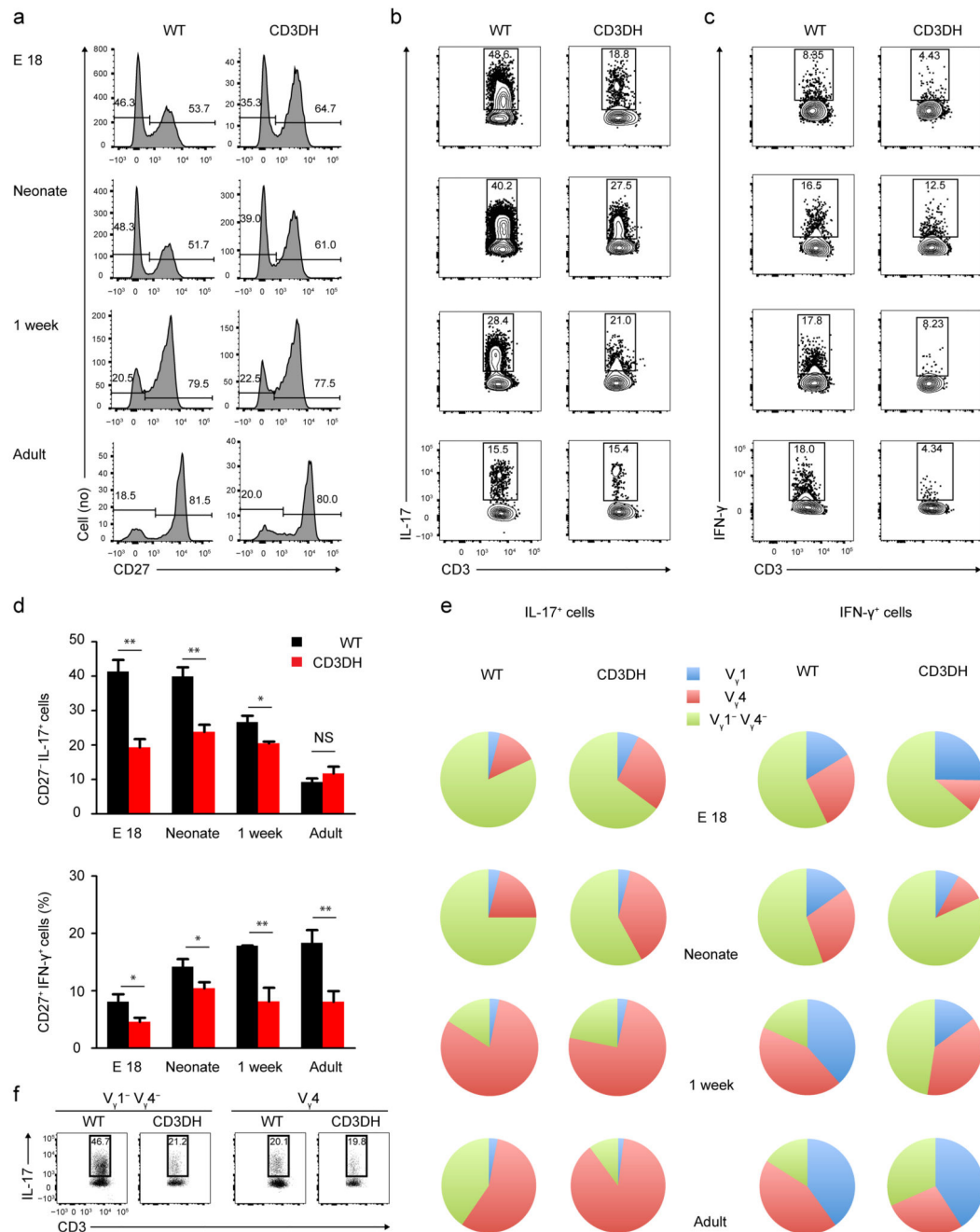


Figure 2. CD3DH mice show impaired differentiation of IL-17⁺ and IFN-γ⁺ γδ T cells within selective windows of TCR V_γ usage

(a-c) Flow cytometry at various developmental stages showing representative surface CD27 expression in gated CD3⁺TCRδ⁺ thymocytes ($n = 10$ per mice group) (a), intracellular IL-17 in CD3⁺TCRδ⁺CD27⁻ thymocytes (b) and IFN-γ expression in CD3⁺TCRδ⁺CD27⁺ thymocytes (c) from WT or CD3DH mice following stimulation with PMA and ionomycin. Data are representative of two to four experiments per developmental stage. Numbers indicate the % cells in the marked region. (d) Percent CD27⁻IL-17⁺ (top) and CD27⁺IFN-γ⁺

(bottom) $\gamma\delta$ T cells in WT and CD3DH mice ($n = 5$ per group) as determined in (b) and (c), respectively. Data shown are the mean \pm s.d. * $P < 0.05$; ** $P < 0.01$ (Student's t -test). (e) $V\gamma$ usage by CD27⁻IL-17⁺ or CD27⁺IFN- γ ⁺ $\gamma\delta$ T cells at various developmental stages ($n = 7$ per group), as determined by flow cytometry. (f) Flow cytometry showing intracellular IL-17 expression in CD3⁺TCR δ ⁺CD27⁻ thymocytes from E18 WT or CD3DH mice following stimulation with PMA and ionomycin. Numbers indicate % cells in the marked region.

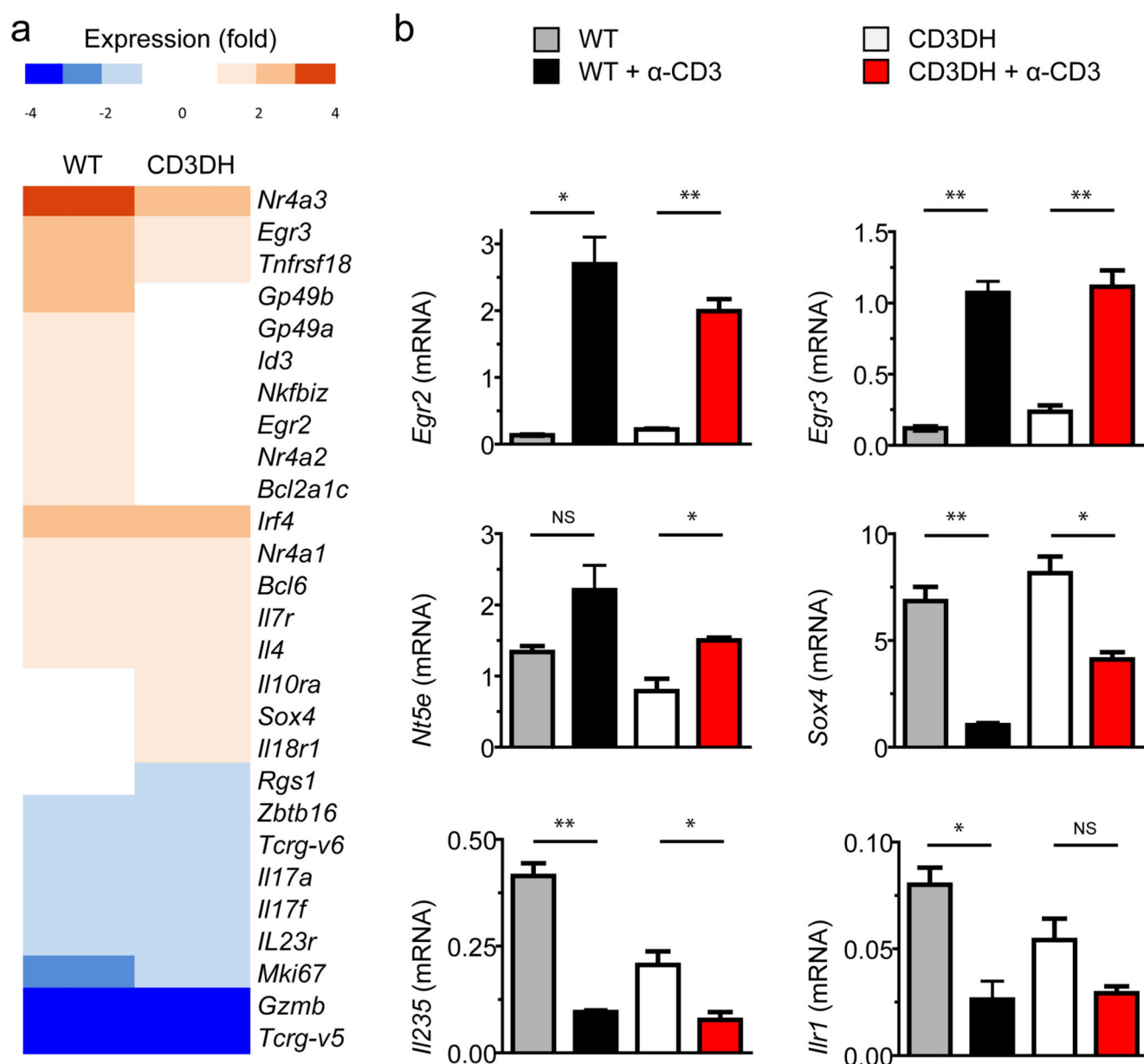


Figure 3. Transcriptional signatures of TCR signal strength in $\gamma\delta$ thymocytes

(a) Microarray heatmap of differentially expressed genes during ontogeny in sorted $CD3^+TCR\delta^+$ $\gamma\delta$ thymocytes of WT or CD3DH mice (>2-fold adult/fetal between week 5-7 and E18). (b) Fold expression by real-time RT-PCR (in arbitrary units normalized to the housekeeping gene *Hprt*) of *Egr2*, *Egr3*, *Nt5e* (encoding CD73), *Sox4*, *Il23r* and *Ilr1* genes by sorted $CD3^+TCR\delta^+$ $\gamma\delta$ thymocytes from WT or CD3DH mice before and after 16h stimulation with α -CD3 ϵ mAb (10 μ g/ml). Data shown are the mean \pm s.d. * P < 0.05; ** P < 0.01 (Student's *t*-test).

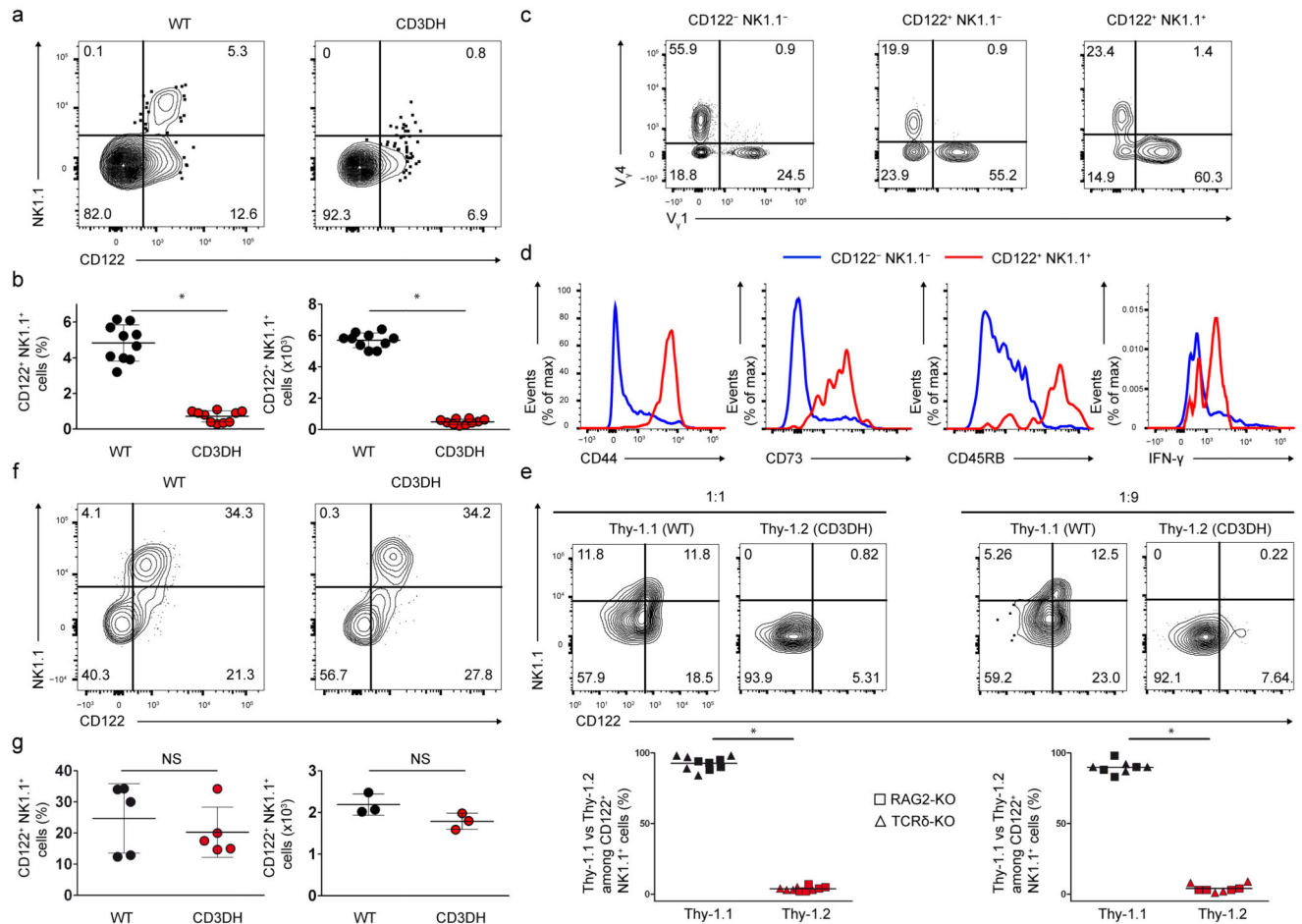


Figure 4. CD3DH mice lack IFN- γ hi CD122⁺ NK1.1⁺ thymocytes that are rescued by CD3 crosslinking *in vivo*

(a) Flow cytometry showing representative NK1.1 vs CD122 expression in TCR δ ⁺CD3⁺CD27⁺ thymocytes isolated from adult WT or CD3DH mice ($n = 10$ per group). Numbers indicate % cells in each quadrant. (b) Frequencies (left) and total numbers (right) of TCR δ ⁺CD3⁺CD27⁺CD122⁺NK1.1⁺ thymocytes. Each dot represents an individual mouse; bars indicate the mean \pm s.d. * $P < 0.01$ (Student's t -test) throughout. (c, d) Flow cytometry showing representative V γ 4 vs V γ 1 chain usage (c) and surface CD44, CD73, CD45RB or intracellular IFN- γ production (d) by the indicated gated TCR δ ⁺CD3⁺CD27⁺ thymocyte subsets from adult WT mice ($n = 5$ per group). Data are representative of at least three independent experiments. (e) Flow cytometry showing representative NK1.1 vs CD122 expression (top) within Thy-1.1⁺ (WT-derived) or Thy-1.2⁺ (CD3DH-derived) fractions (bottom) of TCR δ ⁺CD3⁺CD27⁺CD122⁺NK1.1⁺ thymocytes from 1:1 or 1:9 mixed bone marrow chimeras. Each symbol indicates one host, either RAG2^{-/-} (squares) or TCR δ ^{-/-} (triangles). (f, g) Flow cytometry showing representative NK1.1 vs CD122 expression (f) and % (left) and numbers (right) of TCR $\gamma\delta$ ⁺CD3⁺CD27⁺ CD122⁺NK1.1⁺ thymocytes (g) in WT or CD3DH mice, 5 days after i.p. injection of α -CD3 mAb 17A2 ($n = 3$ per group). Each dot represents an individual mouse; bars indicate the mean \pm s.d.

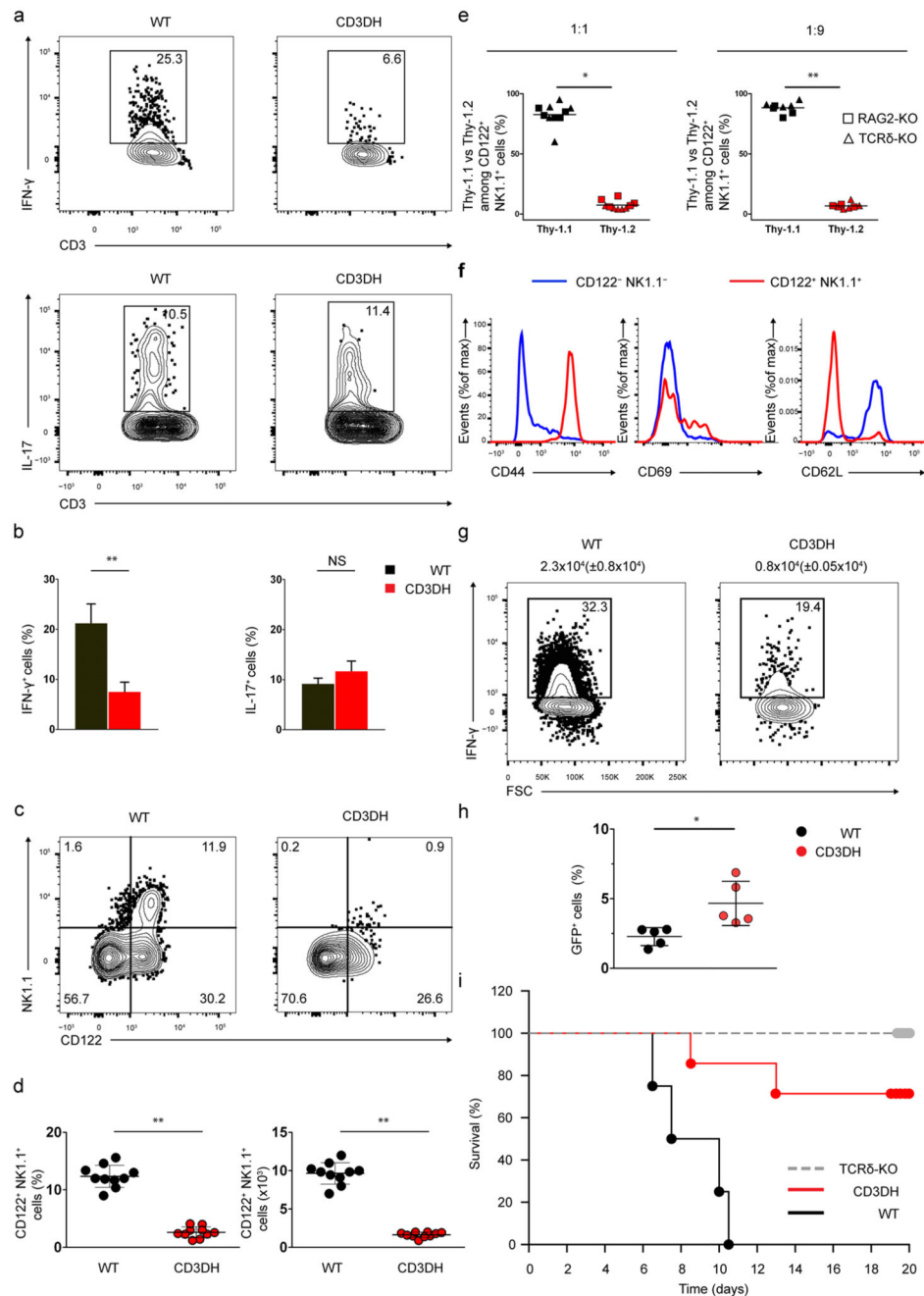


Figure 5. CD3DH mice show reduced peripheral IFN- γ ⁺ γ δ T cells and are resistant to cerebral malaria

(a,b) Intracellular IFN- γ (top) or IL-17 (bottom) expression in CD27⁺ or CD27⁻ TCR δ ⁺CD3⁺ adult mice splenocytes, respectively, stimulated with PMA and ionomycin (a). Numbers indicate % of cells in the marked region, which are shown for $n = 5$ per group in (b). (c, d) NK1.1 vs CD122 expression in TCR δ ⁺CD3⁺CD27⁺ adult mice splenocytes (c). Numbers indicate % of cells in each quadrant, which are shown in (d) for $n = 20$ per group as % (left) or total numbers (right). (e) Thy-1.1 (WT-derived) vs Thy-1.2 (CD3DH-derived)

fractions among $\text{TCR}\delta^+\text{CD3}^+\text{CD27}^+\text{CD122}^+\text{NK1.1}^+$ splenocytes from 1:1 or 1:9 mixed WT:CD3DH BM chimeras. Each symbol indicates one host, either $\text{RAG2}^{-/-}$ (squares) or $\text{TCR}\delta^{-/-}$ (triangles). **(f)** Comparative surface expression of the indicated markers in $\text{CD122}^-\text{NK1.1}^-$ vs $\text{CD122}^+\text{NK1.1}^+$ cells gated on WT $\text{TCR}\gamma\delta^+\text{CD3}^+\text{CD27}^+$ splenocytes. **(g, h)** Intracellular IFN- γ expression (after PMA and ionomycin stimulation) in $\text{TCR}\gamma\delta^+\text{CD3}^+\text{CD27}^+$ splenocytes sorted 5 days after infection with *Plasmodium berghei* ANKA sporozoites. Numbers above plots indicate mean \pm s.d. absolute counts of IFN- γ^+ $\gamma\delta$ cells (g). Parasitemia as % blood GFP^+ cells 5 days after infection (h). **(i)** Survival curves of $n = 10$ mice infected as in (g) in two independent experiments. Data in (a) and (e) are representative of $n = 3$ independent experiments. Error bars indicate s.d. of the mean and dots represent individual mice throughout. * $P < 0.05$, ** $P < 0.01$ (Student's t -test).